Int. J. Heat Mass Transfer. Vol. 29, No. 5, pp. 777–784, 1986
Printed in Great Britain

0017–9310/86 $3.00 + 0.00
Pergamon Journals Ltd.

Local heat transfer from a square prism to an airstream

T. IGARASHI

Department of Mechanical Engineering, The National Defense Academy, Yokosuka 239, Japan

(*Received* 14 *August* 1985 *and in final form* 4 *December* 1985)

Abstract—Experimental investigations on the fluid flow and the local heat transfer from a square prism at angle of attack to an airstream were carried out in the range $1.1 \times 10^4 \leqslant Re \leqslant 5.3 \times 10^4$. Characteristics of the local and average heat transfer on each face were made clear in connection with the flow characteristics. The heat transfer coefficients in the reattachment region and that on the rear face are examined. The average heat transfer coefficients on the rear face are related to the r.m.s. fluctuating pressure and divided into two groups: perfect separation type and reattachment type.

1. INTRODUCTION

IN A PREVIOUS paper [1], the author reported the average heat transfer coefficients from a square prism with angles of attack to an oncoming airstream; the coefficients were measured in the range $5.6 \times 10^3 \leqslant Re \leqslant 5.6 \times 10^4$. The Reynolds number was based on the length of a side of the prism. It was clarified that the average heat transfer is closely connected with the characteristics of the flow around the prism, that is, it increases directly with increases in the values of the reciprocal of the length of vortex formation region, the reciprocal of Strouhal number, base pressure parameter, drag and lift coefficient and fluctuating pressure coefficient. The average heat transfer coefficients at the angles of attack $\alpha = 0°$ and 45° were as high as 40% of the values of Hilpert [2]. His result is so familiar as to be quoted in the textbook by Jakob [3]. It should be pointed out here that the characteristic lengths in Nusselt number and Reynolds number, quoted in several textbooks [4, 5], is not the diameter of a circular tube of equal exposed surface, but the projected length in the direction of the main flow.

In the present paper, the characteristics of the local heat transfer around a square prism under the condition of a constant heat flux, will de described. The local and average heat transfer coefficients on the front face, the reattachment region on the side face, and the side and the rear faces in separated regions are discussed in connection with the characteristics of the flow around the prism of ref. [6].

2. EXPERIMENTAL APPARATUS AND PROCEDURE

The configuration of a model is illustrated in Fig. 1. The wind tunnel used in the present work is the same as that employed in the previous one by the author [1]. The freestream velocity ranged from 6 to 28 m s^{-1}, and the turbulence intensity in this range was 0.5%. The Reynolds number based on the length of a side of a prism, $d = 30$ (29.2) mm, was in the range $1.2 \times 10^4 \leqslant Re \leqslant 5.6 \times 10^4$. The whole surface of the test prism was covered with a stainless steel sheet of 0.02 mm in thickness for the local heat transfer measurement under the condition of a constant heat flux. The accuracy of measurements was remarked in the previous paper [1]. The local and average heat transfer on each face were discussed in connection with the time-averaged and fluctuating pressure distributions as well as the oil-flow patterns on the reattachment face obtained in ref. [6].

3. RESULTS AND DISCUSSION

3.1. *Local heat transfer and flow characteristics*

3.1.1. *Flow pattern.* Concerning the behavior of a shear layer separated from the leading edge corner of a square prism on the side face, the flow patterns around the prism are classified into four types [6]:

I. $0° \leqslant \alpha \leqslant 5°$, perfect separation and symmetric flow type
II. $5° < \alpha \leqslant 13°$, perfect separation and unsymmetric flow type
III. $14° \leqslant \alpha \leqslant 35°$, reattachment flow type
IV. $35° < \alpha \leqslant 45°$, wedge flow type.

An example of flow pattern around the prism is illustrated in Fig. 2. Typical surface flow patterns on the side face AB are shown in Fig. 3. For a perfect

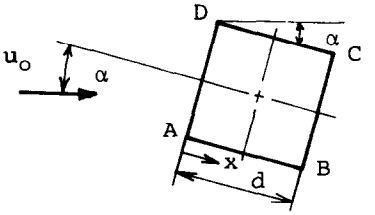

FIG. 1. Flow geometry.

NOMENCLATURE

C constant
Cp, Cp_b pressure coefficient and base pressure coefficient
Cp' r.m.s. coefficient of fluctuating pressure, $\Delta p/0.5\rho u_0^2$
d length of a side of a square prism
h, $\bar{h}$ local and average heat transfer coefficients
K base pressure parameter, $(1-Cp_b)^{0.5}$
Nu, $\overline{Nu}$ local and average Nusselt numbers, hd/λ, $\bar{h}d/\lambda$
Δp r.m.s. of fluctuating pressure
Re Reynolds number, $u_0 d/\nu$
u_0 freestream velocity
u_s velocity along freestream line at separation point, ku_0
X_R, X_S distances from leading edge to reattachment point and separation point on reattachment face.

Greek symbols
α angle of attack
λ thermal conductivity of fluid
ν kinematic viscosity of fluid
ρ density of fluid.

Subscripts
b rear face
f front face
R reattachment point
r rear stagnation point
s side face.

separation type shown in patterns I and II, after the shear layer separated from the edge corner A rolled up, it reattaches on the rear face BC, and passes back around the trailing edge corner B, then reattaches at the point R on the side face AB. The oil-flow patterns show the reattachment and the flow separation at the point S. For the pattern III, the shear layer reattaches directly at the point R on the side face AB. A clear reattachment region appears, and the separation bubble becomes particularly evident. For the pattern IV, there is no separation, because the flow is a wedge flow.

3.1.2. *Local heat transfer.* The variations of the distributions of the local heat transfer coefficient around a square prism with α are shown in Figs. 4(a) and (b). For $0° \leqslant \alpha \leqslant 12°$, there is little effect of α on the coefficients on the front face DA and the lower side face AB. On the other hand, the coefficients on the rear face BC and the upper side face CD are considerably decreased with an increase in α. The front and the rear faces have uniform distributions, which are equivalent to respective faces for a flat plate [9]. The value on the rear face is higher than that on the front one. On the lower side face the value near the trailing edge corner B is higher than that on the rear face because of the reattachment of the reverse flow, and it decreases rapidly toward the separation point X_s. Beyond $\alpha = 15°$, the coefficient on the lower side face AB increases remarkably owing to the reattachment of the shear layer and the value has a maximum at the reattachment point X_s. The maximum value increases and the location X_s moves toward the leading edge corner A with an increase in α. The values on the faces BC and CD in the separated region have a maximum at the corner C.

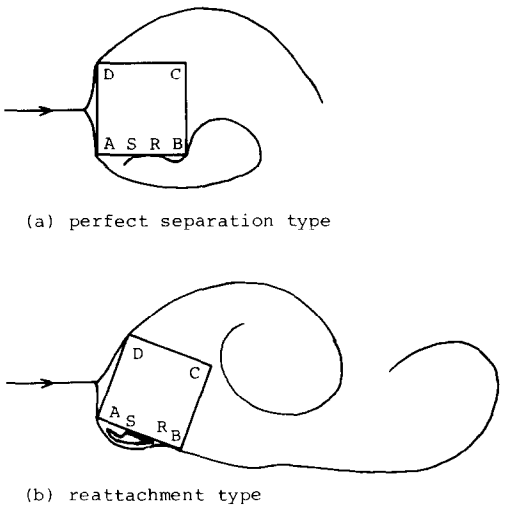

FIG. 2. Typical flow pattern around a square prism.

3.1.3. *Mean and fluctuating pressure.* The mean and fluctuating pressure distributions are shown in Figs. 5 and 6, respectively. For the pattern I, the two profiles on the side faces AB and CD are not symmetric, respectively. For the pattern III, these profiles on the faces BC and CD are symmetric with respect to the corner C, respectively. In the separated region, the larger the value of $-Cp$, the larger is the value of Cp'. The variations of these profiles on the reattachment face AB are peculiar, that is, the value of Cp has a maximum and that of Cp' a minimum at the reattachment point X_R. On the other hand, the profile of heat transfer shown in Fig. 4(b) has a maximum at a point near X_R and a minimum at a point near X_s.

3.1.4. *Dependency on Reynolds number.* The dependencies of the local Nusselt numbers on the Reynolds number for the each face of the prism were examined. The Nusselt number on the front face is expressed by $Nu_f \propto Re^{1/2}$ for all patterns, because a laminar boundary layer is formed on this face. For the side face AB, the Nusselt numbers of the patterns I, II,

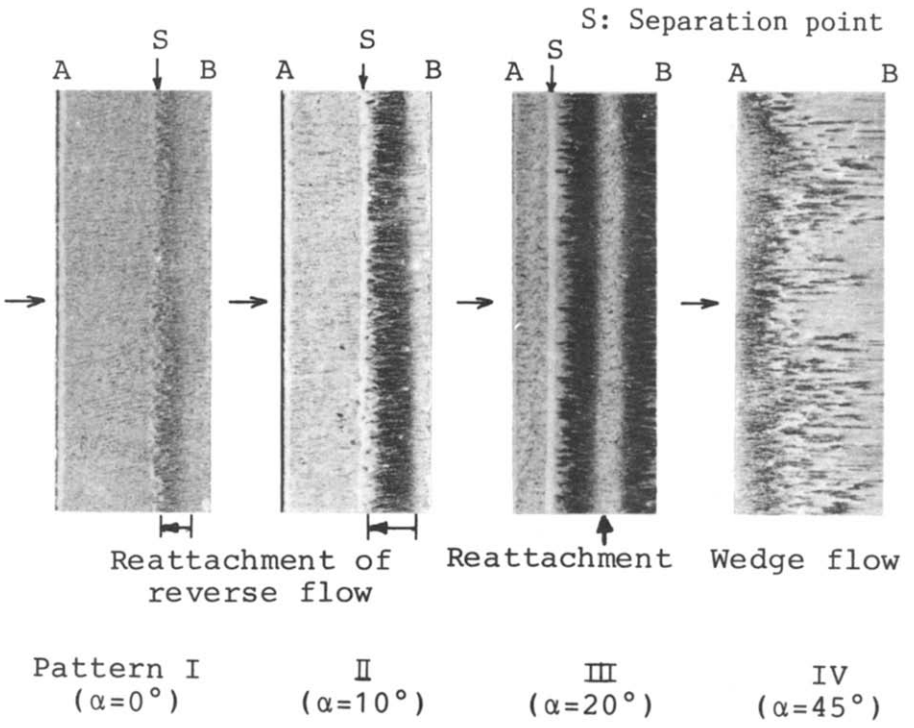

FIG. 3. Surface oil flow pattern on lower face at $Re = 3.7 \times 10^4$.

III and IV are approximately expressed by $Nu_s \propto Re^{0.80}$, $Re^{0.6\sim2/3}$, $Re^{2/3}$ and $Re^{1/2}$, respectively. In pattern IV the face AB becomes the front face with respect to the main flow. The reverse flow or the separated shear layer reattaches onto the face AB, thus the dependency of the local Nusselt number on the Reynolds number varies depending upon the location and is very complicated. The Nusselt numbers on the faces BC and CD in the separated region are given by $Nu_b \propto Re^{2/3}$ for all patterns.

3.2. *Average heat transfer on each face*

Figure 7 shows the average heat transfer coefficient on each face of the prism at $\alpha = 0°$. The coefficient on

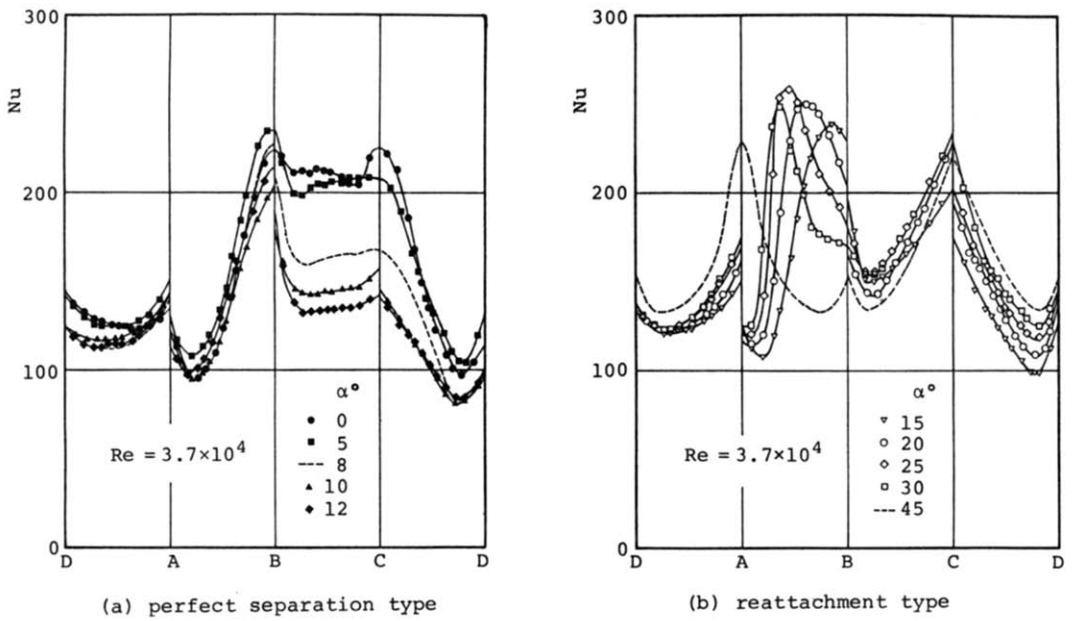

FIG. 4. Local heat transfer distribution: (a) $\alpha = 0$–$12°$; (b) $\alpha = 15$–$45°$.

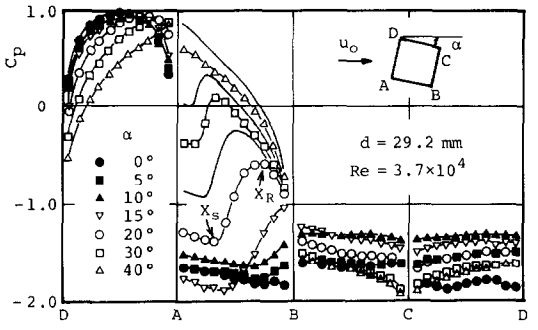

FIG. 5. Pressure distribution.

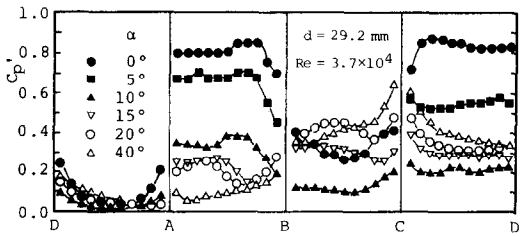

FIG. 6. Distribution of r.m.s. fluctuating pressure.

the front face satisfies the same relation as that for a laminar boundary layer, and those on the side face and on the rear face satisfy the same relation as that for a separated flow region. These are given by

$$\text{face DA:} \qquad \overline{Nu}_f = 0.64\, Re^{1/2} \tag{1}$$

$$\alpha = 0^\circ \text{ faces AB and CD:} \qquad \overline{Nu}_s = 0.131 Re^{2/3} \tag{2}$$

$$\text{face BC:} \qquad \overline{Nu}_b = 0.173 Re^{2/3}. \tag{3}$$

The variations of the average heat transfer on each face with α are shown in Figs. 8(a)–(c). The heat transfer on the front face DA is given by

$$0^\circ \leqslant \alpha \leqslant 45^\circ; \quad \text{face DA:} \quad \overline{Nu}_f = C_f Re^{1/2}. \tag{4}$$

For the perfect separation type, the constant C_f is 0.64, and for the reattachment and the wedge types, these are 0.67 and 0.72, respectively. For the reattachment face AB, the average heat transfer coefficient is given by

$$10^\circ \leqslant \alpha \leqslant 20^\circ; \quad \text{face AB:} \quad \overline{Nu}_s = C_s Re^{2/3}. \tag{5}$$

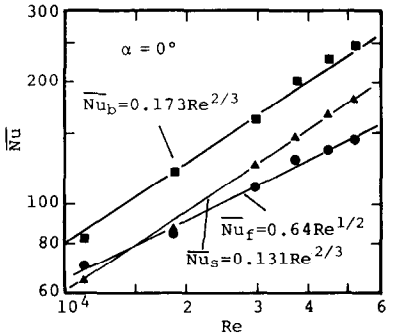

FIG. 7. Comparison of average heat transfer on each face at $\alpha = 0^\circ$.

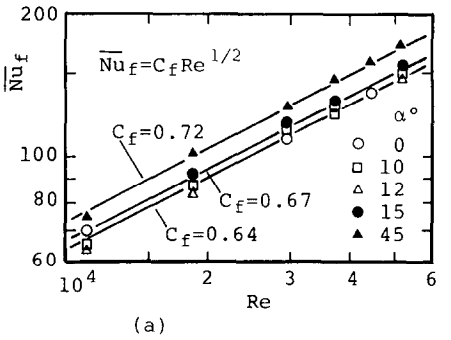

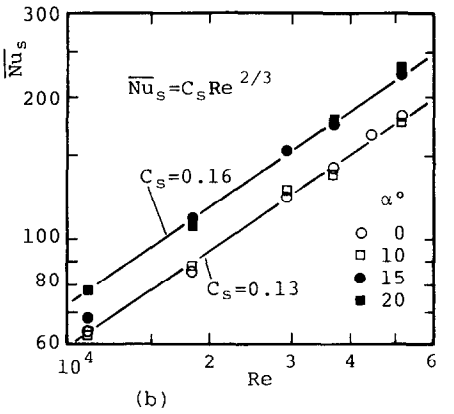

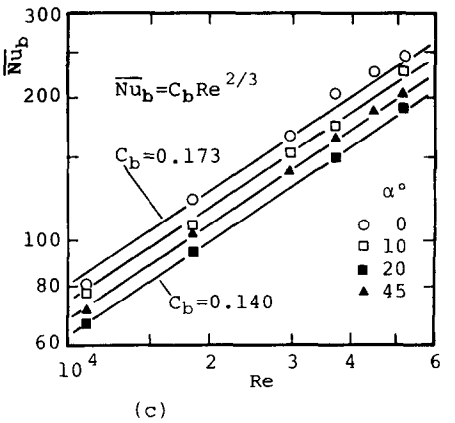

FIG. 8. Average heat transfer on each face: (a) front face DA; (b) lower side face AB; (c) rear face BC.

At $\alpha = 10^\circ$ without reattachment of the shear layer, the constant C_s is 0.13. On the other hand, at $\alpha = 15^\circ$ and 20° with reattachment, the constants are 0.16. The average heat transfers on the rear face BC and on the upper side face CD are given by

$$0^\circ \leqslant \alpha \leqslant 45^\circ \qquad \text{face BC:} \quad \overline{Nu}_b = C_b Re^{2/3}, \tag{6}$$

$$\text{face CD:} \quad \overline{Nu}_s = C_s Re^{2/3}. \tag{7}$$

The variations of the constants C_b and C_s with angles of attack α are shown in Fig. 9. The values of C_b is higher than that of C_s regardless of α, but the difference decreases with an increase in α. The two constants have

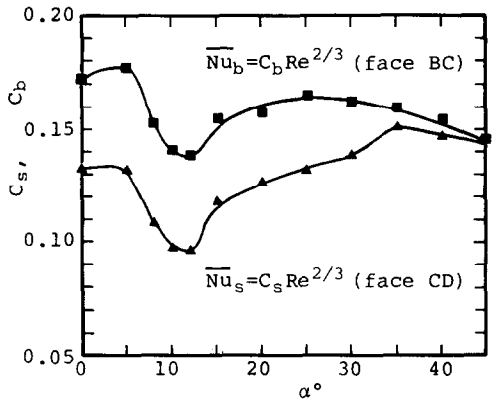

FIG. 9. Variations of average heat transfer on the faces in separated region with angle of attack.

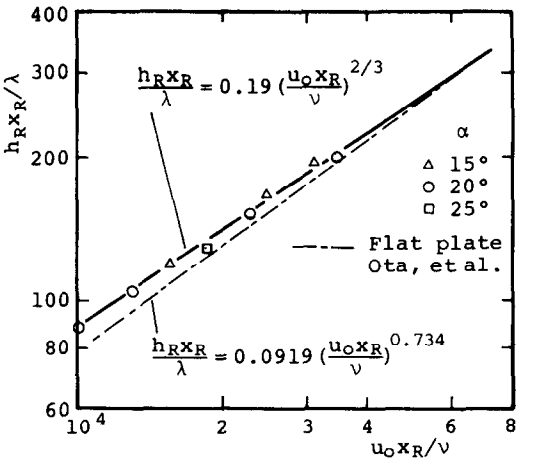

FIG. 10. Correlation of reattachment Nusselt numbers vs Reynolds numbers.

the minimum at $\alpha = 12°$ and show similar tendencies to those of the flow characteristics described in ref. [1]. That is, the trends are similar to those of d/L_v, $1/S$, C_D and Cp', where L_v is the longitudinal length of vortex formation region, S is the Strouhal number and C_D is the drag coefficient. At this angle of $\alpha = 12°$, the vortex formation region L_v is shifted to the most downstream side and the wake width has a minimum. Then the values of K, C_D, Cp' has a minimum and that of S has a maximum.

3.3. *Heat transfer at reattachment point*

According to Ota *et al.* [7], the correlation between the reattachment Nusselt number and the Reynolds number at the reattachment point on blunt flat plates is independent of the nose shape, when the reattachment length is employed as the reference length. They have presented the following empirical formula

$$h_RX_R/\lambda = 0.0919(u_0X_R/\nu)^{0.734}. \quad (8)$$

In this work, the maximum heat transfer coefficients on the reattachment face for $15° \leqslant \alpha \leqslant 25°$ were arranged in the same way as that mentioned above. As shown in Fig. 10, the results obtained can be expressed as

$$h_RX_R/\lambda = 0.19(u_0X_R/\nu)^{2/3}. \quad (9)$$

Equation (9) fits quantitatively with equation (8) and the exponent of Reynolds number, 2/3, is in fair agreement with that behind a double step, obtained by Seki *et al.* [8].

3.4. *Heat transfer on rear face*

In the case of patterns I and II of the perfect separation type, the local heat transfer coefficients on the rear face BC were reasonably constant. The coefficients were compared with the local heat transfer coefficients on the rear faces for a flat plate [9], a semi-circular cylinder [9] and a wedge (an equilateral triangular prism) [10], in which individual coefficients also were reasonably constant. As shown in Fig. 11, these local and average heat transfer coefficients regardless of the configuration are given as

$$\overline{Nu}_b = 0.17Re^{2/3}. \quad (10)$$

The above empirical formula agrees closely with the following semi-theoretical equation for the heat transfer on the rear surface of bluff bodies [11]

$$\overline{Nu}_b = 0.10[2/(d_w/d)]^{1/3}(KRe)^{2/3}. \quad (11)$$

3.5. *Correlation between heat transfer and fluctuating pressure in separated regions*

In the previous papers [12, 13], it has been clarified that the r.m.s. value of fluctuating pressure at the rear stagnation point or at the separation point, Δp_r and Δp_s, are the most dominating factors of the heat transfer in the separated region of a circular cylinder by controlling the shear layer separated from the cylinder and by controlling the wake. Namely, the local and average heat transfer coefficients on the rear surface of cylinder with and without wake controls are correlated with values of Δp_s and Δp_r. After that, it becomes clear that this relation holds regardless of the diameter of the cylinder [14]. The heat transfer coefficient at the rear stagnation point is related to the r.m.s. value of

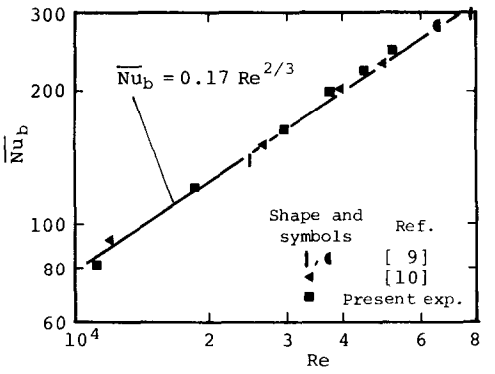

FIG. 11. Heat transfer on rear face.

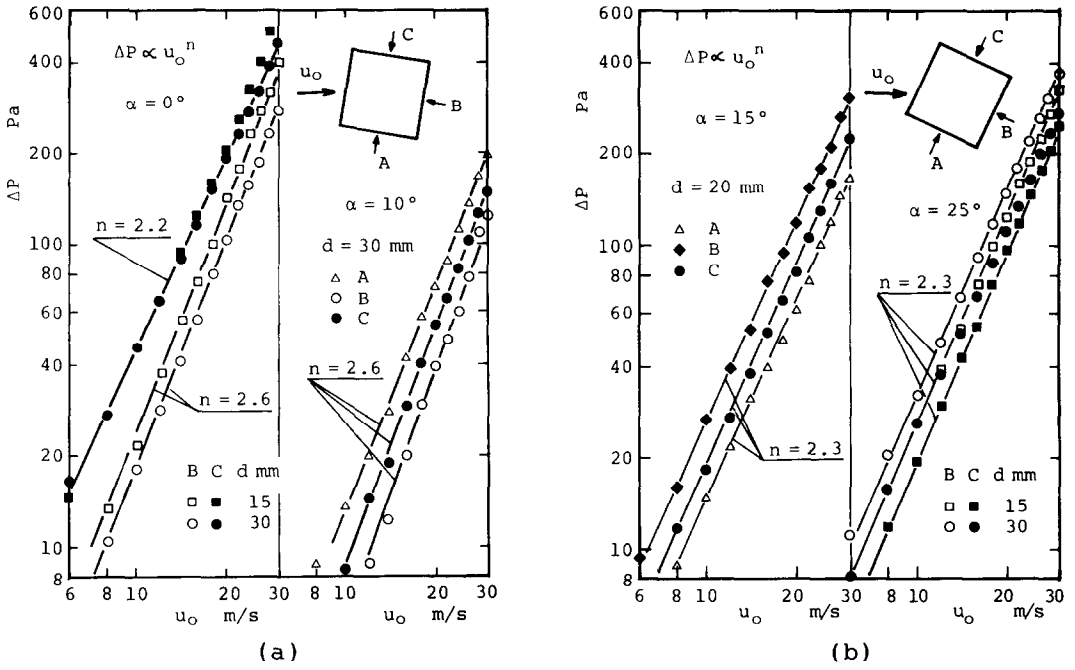

FIG. 12. Correlation of Δp vs u_0.

fluctuating pressure as follows:

$$h_r = C\Delta p_r^{0.33}. \quad (12)$$

$$Cp_r' = \Delta p_r/0.5\rho u_0^2 = 5.35 \times 10^{-4} Re^{0.6}. \quad (13)$$

Further, a similar correlation was found for a circular cylinder with a two-dimensional slit placed along the diameter [15]. In light of the above, measurements of the r.m.s. values of fluctuating pressure, Δp, at the mid-points of the faces in separated region of a square prism were performed for various values of freestream velocity u_0 [6]. The results obtained are shown in Figs. 12(a) and (b). They are represented by the following relations

$$\alpha \leqslant 13° \text{ (perfect separation type)}: \quad \Delta p \propto u_0^{2.6} \quad (14)$$

$$\alpha \geqslant 14° \text{ (reattachment type)}: \quad \Delta p \propto u_0^{2.3}. \quad (15)$$

However, the correlation for the side face of the pattern I of the perfect separation type alone is expressed by $\Delta p \propto u_0^{2.2}$. The difference in values of the above exponent corresponds to those of the exponent of Reynolds number against heat transfer coefficient, as states in section 3.1.4.

The relation between the average heat transfer coefficient and the r.m.s. value of fluctuating pressure on the rear face BC in the separated regions was examined. As shown in Fig. 13, the data points plotted lie in two straight lines depending on flow patterns: one is the patterns I and II of perfect separation type, the other is the patterns III and IV of the reattachment flow and wedge flow types, respectively. The average heat transfer coefficient on the rear face $\bar{h}_b$ is related to the r.m.s. value of fluctuating pressure Δp regardless of the attack angle by the following expression

$$\bar{h}_b = C\Delta p^{0.31}. \quad (16)$$

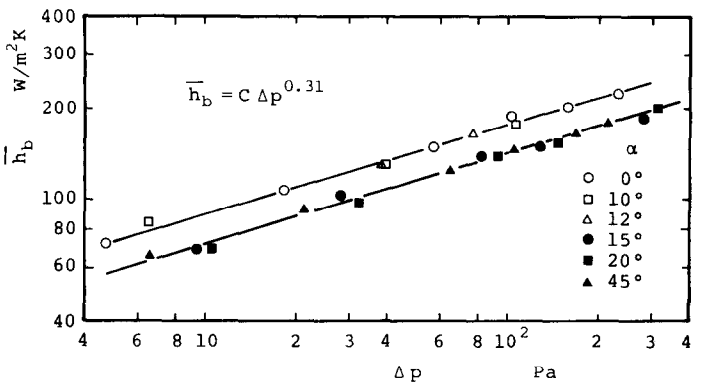

FIG. 13. Correlation of average heat transfer coefficient vs r.m.s. fluctuating pressure on rear face.

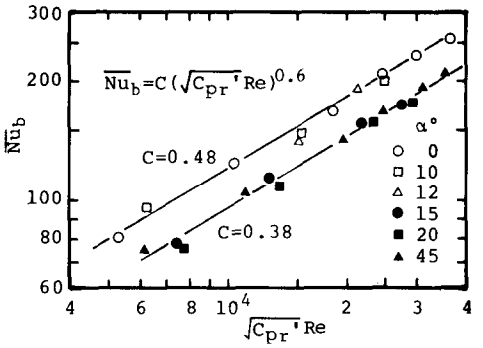

FIG. 14. Average Nusselt number on rear face.

As shown in Fig. 14, the above equation can be rearranged in terms of dimensionless numbers, that is, $\overline{Nu}_b$, Re and Cp'. The relation is formulated as:

$$\alpha \leqslant 12°: \quad \overline{Nu}_b = 0.48(\sqrt{Cp'}Re)^{0.6} \tag{17}$$

$$\alpha \geqslant 15°: \quad \overline{Nu}_b = 0.38(\sqrt{Cp'}Re)^{0.6}. \tag{18}$$

4. CONCLUSIONS

Experimental investigations on the fluid flow and the local heat transfer from a square prism at angles of attack, α, to an airstream were carried out in the range $1.1 \times 10^4 \leqslant Re \leqslant 5.3 \times 10^4$. The main results are summarized as follows:

(1) For $\alpha = 0°$ and 45°, the heat transfer coefficients on the rear surface are higher than those on the front face. In the case of $\alpha = 0°$, the local heat transfer coefficient on the rear face is uniform and is equal to that of flat plate placed normal to an airstream. This is given by

$$\overline{Nu}_b = 0.17Re^{2/3}.$$

(2) The average heat transfer coefficient on the front face is given by

$$\overline{Nu}_f = C_f Re^{1/2},$$

where the constant C_f for the perfect separation flow type, the reattachment flow type and wedge flow type, is 0.64, 0.67 and 0.72, respectively.

(3) The average heat transfer on the lower side face is given by

$$\overline{Nu}_s = C_s Re^{2/3},$$

where the constant C_s for the perfect separation type and the reattachment type is 0.13 and 0.16, respectively.

(4) The maximum local heat transfer coefficient on the reattachment region, h_R, is given by

$$h_R X_R/\lambda = 0.19(u_0 X_R/\nu)^{2/3},$$

where X_R is defined as the distance from the leading edge to the position of reattachment.

(5) The average Nusselt numbers on the rear face and the upper side face are given by

$$\overline{Nu}_b = C_b Re^{2/3}$$

$$\overline{Nu}_s = C_s Re^{2/3}.$$

As illustrated in Fig. 9, the constants C_b and C_s vary with α in the ranges from 0.14 to 0.175 and from 0.095 to 0.15, respectively.

(6) The average heat transfer coefficient on the rear face of the prism in a separated region is related to the r.m.s. value of fluctuating pressure, Δp, at the mid-point of the face by the following expression

$$\overline{h_b} = C\Delta p^{0.31}.$$

The value of constant C can be divided into two groups depending upon α: one is for the perfect separation flow type ($\alpha \leqslant 13°$) and the other is for the reattachment flow and wedge flow types ($\alpha \geqslant 14°$). Furthermore, the factor, Δp, is related to the freestream velocity by equations (14) and (15).

(7) The above correlation between heat transfer and fluctuating pressure is formulated by dimensionless numbers as:

$$\alpha \leqslant 12°: \quad \overline{Nu}_b = 0.48(\sqrt{Cp'}Re)^{0.6}$$

$$\alpha \leqslant 15°: \quad \overline{Nu}_b = 0.38(\sqrt{Cp'}Re)^{0.6}.$$

REFERENCES

1. T. Igarashi, Heat transfer from a square prism to an air stream, *Int. J. Heat Mass Transfer* **28**, 175–181 (1984).
2. M. Jakob, *Heat Transfer*, Vol. 1, p. 562. Wiley,New York (1949).
3. R. Hilpert, Wärmeabgabe von geheizten drähten und rohrem im luftstrom, *Gebiete Ingeurw.* **4**, 215–224. (1933).
4. J. D. Knudsen and D. L. Katz, *Fluid Dynamics and Heat Transfer*, p. 508. McGraw-Hill, New York (1958).
5. J. P. Holman, *Heat Transfer*, 3rd edn, p. 248, McGraw-Hill, New York (1972).
6. T. Igarashi, Characteristics of the flow around a square prism, *Bull. JSME* **27**, 1858–1865 (1984).
7. T. Ota and N. Kon, Heat transfer in the separated and reattached flow over blunt flat plates—effects of nose shape, *Int. J. Heat Mass Transfer* **22**, 197–206 (1979).
8. N. Seki, S. Fukusako and T. Hirata, Effect of stall length on heat transfer in reattached region behind a double step at entrance to an enlarged flat duct, *Int. J. Heat Mass Transfer* **19**, 700–702 (1976).
9. T. Igarashi, M. Hirata and N. Nishiwaki, Heat Transfer in separated flows. Part 1 : experiments on local heat transfer from the rear of a flat plate inclined to an air stream, *Heat Transfer–Jap. Res.* **4**, 11–32 (1975).
10. T. Igarashi and M. Hirata, Heat transfer in separated flows. Part 3 : the case of equilateral triangular prism, *Heat Transfer–Jap. Res.* **6**, 13–39 (1977).
11. T. Igarashi and M. Hirata, Heat transfer in separated flows, *Proc. 5th Int. Heat Transfer Conference*, Vol. 2, pp. 300–304 (1974).
12. T. Igarashi, Fluid flow and heat transfer in the separated region of a circular cylinder with wake control, *Heat Transfer–Jap. Res.* **11**, 1–16 (1982).
13. T. Igarashi, Correlation between heat transfer and

fluctuating pressure in separated region of a circular cylinder, *Int. J. Heat Mass Transfer* **27**, 927–937 (1984).
14. T. Igarashi, Fluid flow and heat transfer in separated region of a circular cylinder, *ASME–JSME Thermal Engng Joint Conference, Proc.*, Vol. 3, pp. 87–93 (1983).
15. T. Igarashi, Fluid flow and heat transfer around a circular cylinder with a two-dimensional slit placed along a diameter, *Trans. Japan Soc. mech. Engrs* **51**, 591–599 (1985).

TRANSFERT THERMIQUE LOCAL POUR UN PRISME CARRE DANS UN COURANT D'AIR

Résumé—L'étude expérimentale du transfert thermique d'un prisme carré placé dans un écoulement d'air est menée pour $1{,}1 \times 10^4 \leqslant \mathrm{Re} \leqslant 5{,}3 \times 10^4$. Les caractéristiques du transfert local et global sur chaque face sont clairement reliées aux caractéristiques de l'écoulement. On examine les coefficients de transfert dans la région de recollement et ceux sur la face arrière. Les coefficients moyens de transfert de chaleur sur l'arrière sont reliés à la moyenne quadratique des fluctuations de pression et ils sont séparés en deux groupes : types parfaits de séparation et de recollement.

LOKALER WÄRMEÜBERGANG VON EINEM QUADRATISCHEN PRISMA AN EINEN LUFTSTROM

Zusammenfassung—Strömung und örtlicher Wärmeübergang an einem quadratischen Prisma, das in bestimmten Winkeln mit Luft angeblasen wird, wurden im Bereich $1{,}1 \times 10^4 \leqslant Re \leqslant 5{,}3 \times 10^4$ experimentell untersucht. Die Eigenschaften des örtlichen und des gemittelten Wärmeübergangs an jeder Seite wurden anhand der Strömungseigenschaften aufgezeigt. Die Wärmeübergangskoeffizienten im Gebiet wiederanliegender Strömung und an der Rückseite wurden untersucht. Die mittleren Wärmeübergangskoeffizienten auf der Rückseite wurden auf den wechselnden Druck bezogen; sie lassen sich in zwei Gruppen einteilen: Strömung mit vollständiger Ablösung und wiederanliegende Strömung.

ЛОКАЛЬНЫЙ ТЕПЛООБМЕН ПРЯМОУГОЛЬНОЙ ПРИЗМЫ С ПОТОКОМ ВОЗДУХА

Аннотация—Экспериментально изучается течение жидкости и локальный теплоперенос от прямоугольной призмы к потоку воздуха при наличии угла атаки в диапазоне чисел Рейнольдса $1{,}1 \times 10^4 \leqslant Re \leqslant 5{,}3 \times 10^4$. Установлено, что локальные и интегральные характеристики теплопереноса на каждой поверхности призмы с параметрами готока. Исследуются коэффициенты теплопереноса в зоне повторного присоединения потока и на поверхности связаны со среднеквадратичными флуктуациями давления и подразделяются на две группы: полного отрыва и повторного присоединения потока.